



Enhanced Star Formation in Both Disks and Ram-pressure-stripped Tails of GASP Jellyfish Galaxies

Benedetta Vulcani¹ , Bianca M. Poggianti¹ , Marco Gullieuszik¹ , Alessia Moretti¹ , Stephanie Tonnesen² ,
Yara L. Jaffé³, Jacopo Fritz⁴ , Giovanni Fasano¹, and Daniela Bettoni¹

¹ INAF-Osservatorio astronomico di Padova, Vicolo Osservatorio 5, IT-35122 Padova, Italy; benedetta.vulcani@inaf.it

² Center for Computational Astrophysics, Flatiron Institute, 162 5th Avenue, New York, NY 10010, USA

³ Instituto de Física y Astronomía, Universidad de Valparaíso, Avda. Gran Bretaña 1111 Valparaíso, Chile

⁴ Instituto de Radioastronomía y Astrofísica, UNAM, Campus Morelia, A.P. 3-72, C.P. 58089, Mexico

Received 2018 August 29; revised 2018 September 26; accepted 2018 October 4; published 2018 October 17

Abstract

Exploiting the data from the Gas Stripping Phenomena in galaxies with MUSE (GASP) program, we compare the integrated star formation rate–mass relation (SFR– M_*) relation of 42 cluster galaxies undergoing ram-pressure stripping (RPS; “stripping galaxies”) to that of 32 field and cluster undisturbed galaxies. Theoretical predictions have so far led to contradictory conclusions about whether or not ram pressure can enhance the star formation (SF) in the gas disks and tails, and until now a statistically significant observed sample of stripping galaxies was lacking. We find that stripping galaxies occupy the upper envelope of the control sample SFR– M_* relation, showing a systematic enhancement of the SFR at any given mass. The star formation enhancement occurs in the disk (0.2 dex), and additional SF takes place in the tails. Our results suggest that strong RPS events can moderately enhance the SF also in the disk prior to gas removal.

Key words: galaxies: clusters: general – galaxies: clusters: intracluster medium – galaxies: evolution – galaxies: general – galaxies: star formation

1. Introduction

Star-forming galaxies falling onto clusters can lose their gas via ram-pressure stripping (RPS) due to their motion through the intracluster medium (ICM; Gunn & Gott 1972). As the gas is lost, the star formation (SF) gets quenched and galaxies eventually become passive.

Observationally, there is increasing evidence for galaxies observed at different stages of stripping. The most spectacular cases, at the peak of the stripping, are the so-called jellyfish galaxies, which show tails with ionized gas and bright blue knots downstream of the disks, indicating substantial SF in their tails, and asymmetric disks of young stars (e.g., Cortese et al. 2007; Smith et al. 2010; Fumagalli et al. 2014; Fossati et al. 2016; Consolandi et al. 2017; Poggianti et al. 2017a).

Few observational works, based on individual objects, have shown that the RPS enhances the SF before quenching it (Crowl et al. 2006; Merluzzi et al. 2013; Kenney et al. 2014), but the effect has never been quantified in a statistically significant sample. On the other hand, Crowl & Kenney (2008) analyzed 10 Virgo galaxies that underwent RPS and found that in general there is, at most, a modest starburst prior to quenching.

Poggianti et al. (2016) assembled a catalog of local gas-stripping candidates, based on B-band images, and found that galaxies showing signs of stripping are preferentially located above the typical star formation rate–mass (SFR– M_*) relation, indicating an SFR excess with respect to normal star-forming galaxies of the same mass. However, their work was based on integrated quantities, and the derivation of SFRs and masses was performed using single-fiber spectroscopy, which is affected by aperture losses that need to be corrected by adopting some assumptions on the mass-to-light ratio gradient. In addition, their SFR measurements did not take into account the fact that the presence of the active galactic nucleus (AGN)

and old (post-AGB) stellar population could alter their estimates (Yan & Blanton 2012; Belfiore et al. 2016). As the fraction of AGN is very high among stripping candidates (Poggianti et al. 2017b; M. Radovich et al. 2018, in preparation) an incorrect treatment of the AGN can affect the SFR– M_* relation.

Using simulations, several groups have been studying the effect of RPS on individual galaxies, often focusing on its impact on the galaxy SFR (e.g., Fujita & Nagashima 1999; Quilis et al. 2000; Roediger & Hensler 2005; Roediger & Brüggén 2006; Tonnesen et al. 2011; Tonnesen & Bryan 2012). Results have been mixed; for example, Kronberger et al. (2008) and Kapferer et al. (2009) found that RPS enhances the overall SFR by up to a factor of 3–10 with respect to an isolated galaxy. Kronberger et al. (2008) found that new stars are mainly formed in the central parts of the disk, but a significant fraction forms in the wake of the galaxy, while Kapferer et al. (2009) found a shift in the SF from the disk to the wake, with net SFR suppression in the disk. The simulations of Tonnesen & Bryan (2012) did not find a significant enhancement of SF in the remaining gas disk, and only low levels of SF in the stripped tails. Roediger et al. (2014) showed that SF enhancements take place only in regions of sufficiently low initial interstellar medium pressure, which will be stripped soon afterward. Bekki (2014) and Steihauser et al. (2016) found that SF enhancement can occur in RPS galaxies, although it depends strongly on the satellite mass, orbit, and inclination angle.

Troncoso Iribarren et al. (2016), using the EAGLE simulation, showed that the SF enhancement occurs only in the half of the galaxy that is facing the cluster center during its infall. J. Fritz et al. 2018, (in preparation) found observational evidence for this result. Analyzing the spatially resolved SFR of jellyfish galaxies in their initial stripping phase, they found an SFR enhancement on the leading side of the galaxy disk. Assuming that galaxies move toward the cluster center, this relative triggering corresponds to the RPS compression.

The physical origin of the enhancement is still not totally understood. In dynamically disturbed clusters extreme RPS events can be abundant (Vijayaraghavan & Ricker 2013; Jaffé et al. 2016; McPartland et al. 2016), and the SFR triggering seems to be higher in merging clusters (but see Fujita & Nagashima 1999, for opposite results). In these environments, galaxies can encounter higher-velocity ICM headwinds after being overrun by the merger shocks. The accompanying enhanced ICM pressure behind the shock could potentially boost the SF in these stripping galaxies (Bekki & Couch 2010; Bekki et al. 2010; Roediger et al. 2014). The higher the compression, the faster the SF quenching (Bekki et al. 2010).

In this Letter we analyze the disk $\text{SFR}-M_*$ relation of stripping and undisturbed galaxies, using integral field unit data covering up to several effective radii from the galaxy disk. Our sample is extracted from GAs Stripping Phenomena in galaxies with MUSE⁵ (GASP), an ESO Large Programme granted 120 hr of observing time with the integral field spectrograph MUSE that was completed in 2018 April. GASP allows us to study galaxies in the local universe in various stages of RPS in clusters (Jaffé et al. 2018), from pre-stripping (undisturbed galaxies), to initial stripping, peak stripping (Bellhouse et al. 2017; Gullieuszik et al. 2017; Poggianti et al. 2017a; Moretti et al. 2018), and post-stripping (Fritz et al. 2017), passive and devoid of gas.

While many single jellyfish galaxies have been already studied in the literature (e.g., Cortese et al. 2007; Smith et al. 2010; Merluzzi et al. 2013; Fumagalli et al. 2014; Fossati et al. 2016; Consolandi et al. 2017), GASP provides us with the unique possibility of looking for trends and performing comparisons in a homogeneous sample, reducing possible biases. Apart from Poggianti et al. (2016), no attempts to place them on the SFR–mass relation have been carried out so far.

We adopt a Chabrier (2003) initial mass function (IMF) in the mass range $0.1-100 M_{\odot}$. The cosmological constants assumed are $\Omega_m = 0.3$, $\Omega_{\Lambda} = 0.7$ and $H_0 = 70 \text{ km s}^{-1} \text{ Mpc}^{-1}$.

2. The Data Sample

The GASP targets are at redshift $0.04 < z < 0.1$, are located in different environments (galaxy clusters, groups, filaments, and isolated) and span a wide range of galaxy stellar masses, from 10^9 to $10^{11.5} M_{\odot}$. They were drawn from the Poggianti et al. (2016) catalog, based on the WINGS (Fasano et al. 2006) and OMEGAWINGS (Gullieuszik et al. 2015) cluster surveys and the Padova Millennium Galaxy and Group Catalog (Calvi et al. 2011). The GASP sample comprises 94 galaxies selected as stripping candidates (64 in clusters and 30 in groups, filaments, or isolated), plus another 20 undisturbed galaxies in clusters or the field selected as a control sample. A complete description of the survey strategy, data reduction, and analysis procedures is presented in Poggianti et al. (2017a, hereafter Paper I).

In this Letter, we have selected cluster members with signs of initial (J0.5), moderate (J1), and extreme (J2) stripping, as well as truncated disks (J3), for a total of 42 galaxies. We disregarded all of the uncertain cases. Details on the stripping stages (Jstage) can be found in Jaffé et al. (2018). We will call this sample “stripping sample.” The subdivision into Jstages aims at distinguishing galaxies in different evolutionary phases

and at different stages of gas stripping. J3 (9.5% of the total) have very little gas left in the disk and are at a later stripping stage than the other galaxies. The J0.5 (9.5%) and J1 (45%) still have significant gas in the disk, and the J2 (36%) display long tails of stripped material.

We have then extracted from the cluster control sample and the field those galaxies that indeed are undisturbed and do not show any sign of environmental effects (RPS, tidal interaction, mergers, gas accretion, etc.) on their spatially resolved SF distribution, for a total of 17 cluster members and 15 field galaxies. While the control sample is relatively small, it ensures control over the systematics that can arise from comparing inhomogeneous samples. Indeed, differences in, for example, assumed cosmology, IMF, luminosity-to-SFR conversions, stellar population models, dust attenuation, and emission line contributions, can lead to differences in derived stellar masses and SFRs as high as a factor of two to three (e.g., Speagle et al. 2014, Davies et al. 2016).

2.1. Observations and Data Reduction

Observations were carried out in service mode with the MUSE spectrograph mounted at the Very Large Telescope (VLT). MUSE has $0''.2 \times 0''.2$ pixels and covers a $1' \times 1'$ field of view. It covers the spectral range between 4800 and 9300 Å sampled at $1.25 \text{ \AA}/\text{pixel}$ with a spectral resolution $\text{FWHM} = 2.6 \text{ \AA}$. Most of the targets were observed with one MUSE pointing, while for some of them two pointings were needed to cover the entire galaxy and the tail. On each pointing, $4 \times 675 \text{ s}$ exposures were taken in clear, dark-time, $< 1''$ seeing conditions.

The data were reduced with the most recent available version of the MUSE pipeline,⁶ as described in Paper I. All datacubes were then averaged filtered in the spatial direction with a 5×5 pixel kernel, corresponding to our worst seeing conditions of $1'' = 0.7-1.3 \text{ kpc}$ at the redshifts of the GASP galaxies (see Paper I for details).

2.2. Data Analysis

The methods used to analyze the GASP datacubes are extensively presented in Paper I. In brief, we corrected the reduced datacube for extinction due to our Galaxy and subtracted the stellar-only component of each spectrum derived with our spectrophotometric code SINOPSIS (Fritz et al. 2017). This tool also provides for each MUSE spaxel many different quantities. Stellar masses, along with errors, are the ones of interest in this Letter.

We then derived emission line fluxes with associated errors using KUBEVIZ (Fossati et al. 2016), an IDL public software. $\text{H}\alpha$ luminosities corrected both for stellar absorption and for dust extinction were used to compute SFRs, adopting the Kennicutt (1998)’s relation: $\text{SFR} (M_{\odot} \text{ yr}^{-1}) = 4.6 \times 10^{-42} L_{\text{H}\alpha} (\text{erg s}^{-2})$. The extinction is estimated from the Balmer decrement assuming a value $\text{H}\alpha/\text{H}\beta = 2.86$ and the Cardelli et al. (1989) extinction law.⁷ As the formal errors obtained by KUBEVIZ are negligible with respect to the uncertainties of the conversion factor from luminosities to

⁵ <http://web.oapd.inaf.it/gasp/index.html>

⁶ <http://www.eso.org/sci/software/pipelines/muse>

⁷ Note that even though we do not take into account the galaxy inclination angles in the computation of the extinction, both the control and the stripping sample have similar distributions and median values.

Table 1
Properties of the Cluster Stripping Galaxy Sample

ID	z	R.A. (J2000)	Decl. (J2000)	Jstage	$M_{*,\text{disk}}$ ($10^{10} M_{\odot}$)	SFR_{disk} ($M_{\odot} \text{ yr}^{-1}$)	SFR_{tot} ($M_{\odot} \text{ yr}^{-1}$)
JO10	0.0471	00:57:41.61	-01:18:43.994	3	5.7 ± 0.8	3.1 ± 0.6	3.1 ± 0.6
JO112	0.0583	03:40:06.02	-54:02:27.300	1	0.41 ± 0.07	0.7 ± 0.1	0.7 ± 0.1
JO113	0.0552	03:41:49.17	-53:24:13.680	1	0.5 ± 0.1	1.7 ± 0.3	1.8 ± 0.3
JO13	0.0479	00:55:39.68	-00:52:35.981	0.5	0.7 ± 0.1	1.5 ± 0.3	$1. \pm 0.3$
JO135	0.0544	12:57:04.30	-30:22:30.313	2	10 ± 2	4.3 ± 0.8	4.3 ± 0.9
JO138	0.0572	12:56:58.51	-30:06:06.284	0.5	0.4 ± 0.1	0.22 ± 0.04	0.23 ± 0.05
JO141	0.0587	12:58:38.38	-30:47:32.200	1	4.8 ± 1	2.5 ± 0.5	2.6 ± 0.5
JO144	0.0515	13:24:32.43	-31:06:59.036	1	3 ± 1	4.0 ± 0.8	4.0 ± 0.81
JO147	0.0506	13:26:49.73	-31:23:45.511	2	11 ± 2	4.5 ± 0.9	4.6 ± 0.9
JO149	0.0438	13:28:10.53	-31:09:50.200	2	0.06 ± 0.02	0.30 ± 0.06	0.42 ± 0.08
JO156	0.0512	13:28:34.46	-31:01:26.777	1	0.4 ± 0.1	0.28 ± 0.06	0.29 ± 0.06
JO159	0.0480	13:26:35.70	-30:59:36.920	1	0.7 ± 0.2	1.2 ± 0.2	1.3 ± 0.3
JO160	0.0483	13:29:28.62	-31:39:25.288	2	1.1 ± 0.3	1.9 ± 0.4	1.9 ± 0.4
JO162	0.0454	13:31:29.92	-33:03:19.576	2	0.27 ± 0.06	0.40 ± 0.08	0.44 ± 0.09
JO171	0.0521	20:10:14.70	-56:38:30.561	2	4.1 ± 0.6	1.4 ± 0.3	1.8 ± 0.4
JO175	0.0468	20:51:17.60	-52:49:21.825	2	3.2 ± 0.5	2.4 ± 0.5	2.5 ± 0.5
JO179	0.0618	21:47:07.07	-43:42:18.221	0.5	0.33 ± 0.09	0.7 ± 0.1	0.7 ± 0.1
JO181	0.0598	22:28:03.80	-30:18:03.812	1	0.12 ± 0.03	0.24 ± 0.05	0.26 ± 0.05
JO194	0.0420	23:57:00.68	-34:40:50.117	2	15.0 ± 3	8 ± 2	9 ± 2
JO197	0.0562	09:06:32.58	-09:31:27.282	1	1.1 ± 0.3	0.8 ± 0.2	0.8 ± 0.2
JO200	0.0527	00:42:05.03	-09:32:03.841	1	7 ± 1	2.3 ± 0.5	2.4 ± 0.5
JO201	0.0446	00:41:30.29	-09:15:45.900	2	6.2 ± 0.8	5 ± 1	6 ± 1
JO204	0.0424	10:13:46.83	-00:54:51.056	2	4.1 ± 0.6	1.5 ± 0.3	1.7 ± 0.3
JO206	0.0511	21:13:47.41	+02:28:34.383	2	9.1 ± 0.9	4.8 ± 0.9	5 ± 1
JO23	0.0551	01:08:08.10	-15:30:41.841	3	0.5 ± 0.1	0.31 ± 0.06	0.31 ± 0.06
JO27	0.0493	01:10:48.56	-15:04:41.611	1	0.32 ± 0.08	0.5 ± 0.1	0.6 ± 0.1
JO28	0.0543	01:10:09.31	-15:34:24.507	1	0.23 ± 0.04	0.15 ± 0.03	0.17 ± 0.03
JO36	0.0408	01:12:59.42	+15:35:29.356	3	6 ± 1	6 ± 1	6 ± 1
JO47	0.0428	01:15:57.67	+00:41:35.938	1	0.40 ± 0.06	0.39 ± 0.08	0.40 ± 0.08
JO49	0.0451	01:14:43.85	+00:17:10.091	1	4.8 ± 0.6	1.4 ± 0.3	1.4 ± 0.3
JO60	0.0622	14:53:51.57	+18:39:06.364	2	2.5 ± 0.6	4.3 ± 0.9	4.5 ± 0.9
JO69	0.0550	21:57:19.20	-07:46:43.794	1	0.8 ± 0.2	1.3 ± 0.3	1.3 ± 0.3
JO70	0.0578	21:56:04.07	-07:19:38.020	1	2.9 ± 0.6	2.6 ± 0.53	2.8 ± 0.5
JO85	0.0354	23:24:31.36	+16:52:05.340	1	4.6 ± 0.9	5 ± 1	6 ± 1
JO95	0.0433	23:44:26.66	+09:06:55.839	1	0.23 ± 0.04	0.37 ± 0.07	0.40 ± 0.08
JW10	0.0718	04:39:18.19	-21:57:49.627	1	1.0 ± 0.2	0.8 ± 0.1	0.8 ± 0.2
JW100	0.0619	23:36:25.06	+21:09:02.529	2	29 ± 7	2.6 ± 0.5	$4. \pm 0.8$
JW108	0.0477	06:00:47.96	-39:55:07.416	3	3.0 ± 0.7	2.2 ± 0.4	2.2 ± 0.4
JW115	0.0725	12:00:47.95	-31:13:41.635	1	0.5 ± 0.1	0.5 ± 0.1	0.5 ± 0.1
JW29	0.0431	12:57:49.48	-17:39:57.095	0.5	0.32 ± 0.06	0.5 ± 0.1	0.5 ± 0.1
JW39	0.0663	13:04:07.71	+19:12:38.486	2	17 ± 3	3.1 ± 0.6	3.6 ± 0.7
JW56	0.0387	13:27:03.03	-27:12:58.205	2	0.11 ± 0.03	0.13 ± 0.03	0.17 ± 0.03

SFR, we assume uncertainties on SFR to be 20% of the values (Kennicutt et al. 2009).

We employed the standard diagnostic diagrams [O III]5007/H β versus [N II]6583/H α to separate the regions powered by SF, Composite (SF+AGN), AGN, and low-ionization nuclear emission line region (LINER) emission. We adopted the division lines by Kewley et al. (2001), Kauffmann et al. (2003), and Sharp & Bland-Hawthorn (2010). To compute SFRs, we considered only the spaxels whose ionized flux is powered by SF or belong to the Composite region defined by Kauffmann et al. (2003).

Both for stellar masses and for SFRs, we computed total integrated quantities by summing the values of all of the spaxels belonging to each galaxy. To determine the galaxy disk, we use the definition of galaxy boundaries developed by M. Gullieuszik et al. (2018, in preparation) and already exploited by Poggianti et al. (2018). For each galaxy, these

boundaries are computed from the map of the stellar continuum in the H α region and from the isophote with a surface brightness 1σ above the average sky background level. Because of the (stellar and gaseous) emission from the stripped gas tails, this isophote does not have an elliptical symmetry. To obtain a symmetric isophote, we fit an ellipse to the undisturbed side of the isophote and replace the isophote on the disturbed side with the ellipse. Everything inside of this isophote represents the galaxy disk, the rest constitutes the galaxy “tail.” Stellar masses are computed only within the galaxy disk, while for SFR we will also contrast disk and total (disk+tail) values.

By definition, control sample galaxies have negligible H α flux (therefore SFR) in the tails. Quantities for the stripping sample are given in Table 1, quantities for the control sample are given in Table 2.

Table 2
Properties of the Control Galaxy Sample

ID	z	R.A. (J2000)	Decl. (J2000)	$M_{*,\text{disk}}$ ($10^{10} M_{\odot}$)	SFR_{disk} ($M_{\odot} \text{ yr}^{-1}$)	SFR_{tot} ($M_{\odot} \text{ yr}^{-1}$)
cluster						
A3128_B_0148	0.0575	03:27:31.09	-52:59:07.655	0.7 ± 0.2	0.7 ± 0.1	0.7 ± 0.14
A3266_B_0257	0.0584	04:27:52.58	-60:54:11.565	0.8 ± 0.2	0.5 ± 0.1	0.5 ± 0.1
A3376_B_0261	0.0506	06:00:13.68	-39:34:49.232	3.4 ± 0.6	2.0 ± 0.4	2.1 ± 0.4
A970_B_0338	0.0591	10:19:01.65	-10:10:36.924	1.2 ± 0.2	0.7 ± 0.1	0.7 ± 0.1
JO102	0.0594	03:29:04.69	-52:50:05.364	1.0 ± 0.2	0.9 ± 0.2	0.9 ± 0.2
JO123	0.0550	12:53:01.03	-28:36:52.584	0.7 ± 0.2	0.25 ± 0.05	0.25 ± 0.05
JO128	0.0500	12:54:56.84	-29:50:11.184	0.8 ± 0.2	0.8 ± 0.2	0.8 ± 0.2
JO17	0.0451	01:08:35.33	+01:56:37.043	1.4 ± 0.3	0.9 ± 0.2	0.9 ± 0.2
JO180	0.0647	21:45:15.00	-44:00:31.188	1.0 ± 0.2	0.42 ± 0.08	0.42 ± 0.08
JO205	0.0448	21:13:46.12	+02:14:20.355	0.33 ± 0.08	0.6 ± 0.1	0.6 ± 0.1
JO41	0.0477	12:53:54.79	-15:47:20.096	1.6 ± 0.3	0.31 ± 0.06	0.31 ± 0.06
JO45	0.0425	01:13:16.58	+00:12:05.839	0.15 ± 0.04	0.11 ± 0.02	0.12 ± 0.02
JO5	0.0648	10:41:20.38	-08:53:45.559	1.9 ± 0.4	1.3 ± 0.3	1.3 ± 0.3
JO68	0.0561	21:56:22.00	-07:54:28.971	1.0 ± 0.2	0.7 ± 0.1	0.7 ± 0.1
JO73	0.0713	22:04:25.99	-05:14:47.041	1.1 ± 0.3	1.0 ± 0.2	1.0 ± 0.2
JO89	0.0423	23:26:00.60	+14:18:26.291	0.5 ± 0.1	0.12 ± 0.02	0.12 ± 0.02
JO93	0.0370	23:23:11.74	+14:54:05.013	3.5 ± 0.5	1.8 ± 0.4	1.9 ± 0.4
field						
P13384	0.0512	10:53:03.15	-00:13:30.932	0.7 ± 0.2	0.6 ± 0.1	0.6 ± 0.1
P15703	0.0424	11:06:33.28	+00:16:48.192	10 ± 2	1.1 ± 0.2	1.1 ± 0.2
P17945	0.0439	11:15:26.45	+00:16:11.586	0.6 ± 0.1	0.49 ± 0.09	0.5 ± 0.1
P19482	0.0407	11:22:31.25	-00:01:01.601	2.2 ± 0.4	1.3 ± 0.2	1.3 ± 0.2
P20769	0.0489	11:27:17.60	+00:11:24.388	0.3 ± 0.1	0.19 ± 0.04	0.20 ± 0.04
P20883	0.0614	11:27:45.41	-00:07:16.580	0.8 ± 0.2	0.37 ± 0.07	0.37 ± 0.07
P21734	0.0686	11:31:07.90	-00:08:07.914	6 ± 1	3.0 ± 0.6	3.1 ± 0.6
P25500	0.0603	11:51:36.28	+00:00:01.929	7 ± 1	2.1 ± 0.4	2.2 ± 0.4
P42932	0.0410	13:10:44.71	+00:01:55.540	3.3 ± 0.6	2.2 ± 0.4	2.2 ± 0.4
P45479	0.0515	13:23:34.73	-00:07:51.673	3.7 ± 0.6	1.8 ± 0.4	1.8 ± 0.4
P48157	0.0614	13:36:01.59	+00:15:44.696	3.9 ± 0.8	2.5 ± 0.5	2.5 ± 0.5
P57486	0.0529	14:11:34.45	+00:09:58.293	0.9 ± 0.2	0.6 ± 0.1	0.6 ± 0.1
P648	0.0661	10:01:27.74	+00:09:18.372	2.8 ± 0.6	1.1 ± 0.2	1.1 ± 0.2
P669	0.0457	10:02:00.62	+00:10:44.299	3.2 ± 0.6	0.7 ± 0.1	0.7 ± 0.1
P954	0.0451	10:02:03.33	-00:12:49.836	0.4 ± 0.1	0.38 ± 0.07	0.38 ± 0.07

3. Results

The main result of this Letter is shown in Figure 1, where the disk $\text{SFR}-M_*$ relation for galaxies at different stages of stripping is shown. These galaxies are compared to the control sample.

In the control sample, field and cluster galaxies occupy the same region of the plot, indicating that undisturbed star-forming galaxies do not feel the environment in which they are embedded yet and that cluster galaxies can be as star-forming as field galaxies, in agreement with many literature results (e.g., Paccagnella et al. 2016). The relation is qualitatively in agreement with the one shown in Poggianti et al. (2016), even though a meaningful quantitative comparison is prevented by the differences on the data acquisition and analysis, as discussed in the Introduction (see Boselli et al. 2015; Richards et al. 2015; and Gavazzi et al. 2018 for a discussion on the comparison between nuclear and total spectra).

It seems immediately clear, instead, that stripping galaxies populate the upper envelope of the control sample relation. J1 and J2 galaxies, which are the objects with the longest tails, deviate the most. Nonetheless, even truncated disks (J3) and galaxies at initial stripping (J0.5) do show a significant enhancement of the SF. A mass segregation effect is also visible: J2 galaxies are also the most massive ones.

Results are not driven by the galaxy inclination angles: no significant trends are observed when inclination is taken into account (plot not shown).

To place the differences between the two samples on a statistical ground, we fit the data points to obtain the best-fit relations, using a least square fitting method that takes into account uncertainties on both axis. When fitting the control sample, we assume both parameters free, when instead we fit the stripping sample we use the slope of the control sample, to allow a fairer comparison of the intercepts. We do not attempt to fit separately galaxies belonging to different classes, due to the low number statistics.

The control and stripping samples are described by relations that are different at more than 2σ levels, and the difference between the two fits is 0.2 dex.

This result indicates that galaxies feeling the effect of RPS show a significant enhancement of the SFR on the disk of the galaxy, with respect to control sample galaxies of similar mass. Differences are better seen in Figure 2, where the distribution of the difference between the SFR of each galaxy and the value derived from the control sample fit given the galaxy mass is shown. As the fit was carried out taking into account the uncertainties in both M_* and SFR, the control sample distribution does not peak exactly at zero. A tail of galaxies with reduced SFR is visible in the control sample. Two of these

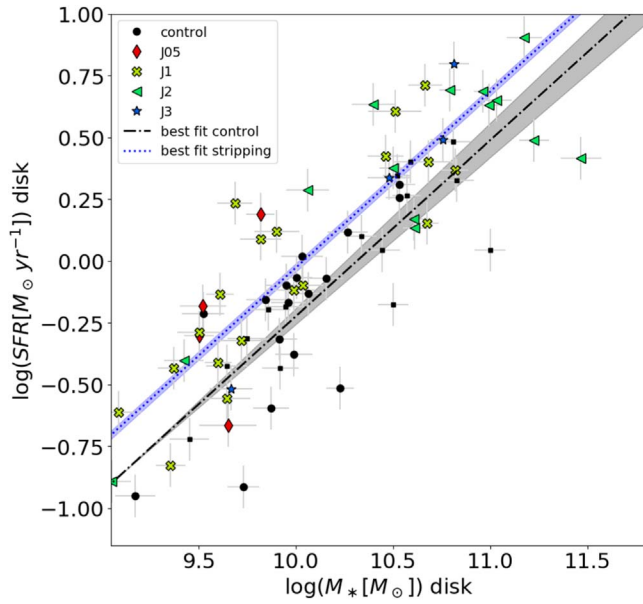


Figure 1. Disk SFR–mass relation for stripping and control sample galaxies. Black symbols refer to the control sample, with dots representing galaxies in clusters, squares galaxies in the field. Colored symbols represent stripping galaxies, with red diamonds representing galaxies at initial stripping (J0.5), yellow crosses stripping galaxies (J1), green triangles peak stripping galaxies (J2), and light blue stars truncated disks (J3). Black dashed–dotted line and shaded gray area show the best fit for the control sample, blue dashed line and shaded blue area show the best fit for the stripping sample, adopting the same slope as the control sample.

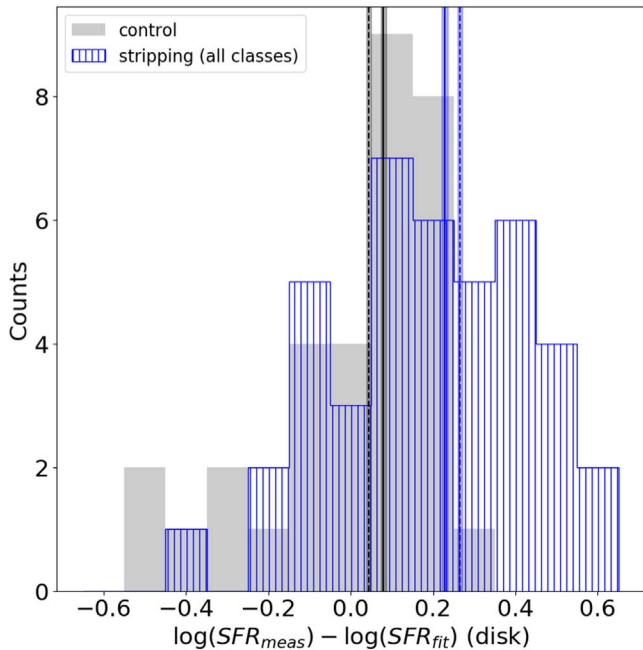


Figure 2. Distributions of the differences between the galaxy SFRs and their expected value according to the fit to the control sample, given their mass. Black and gray colors refer to the control sample, blue color refers to the stripping sample. Dashed lines give mean values, solid lines median values.

galaxies belong to the field, two to the cluster sample. Even though their current SF map does not show anomalies, their spatially resolved SF histories obtained from SINOPSIS show that the radial extent of the SF has reduced in the recent past, suggesting that these galaxies are transitioning from being star-forming to passive (Paccagnella et al. 2016). Removing these

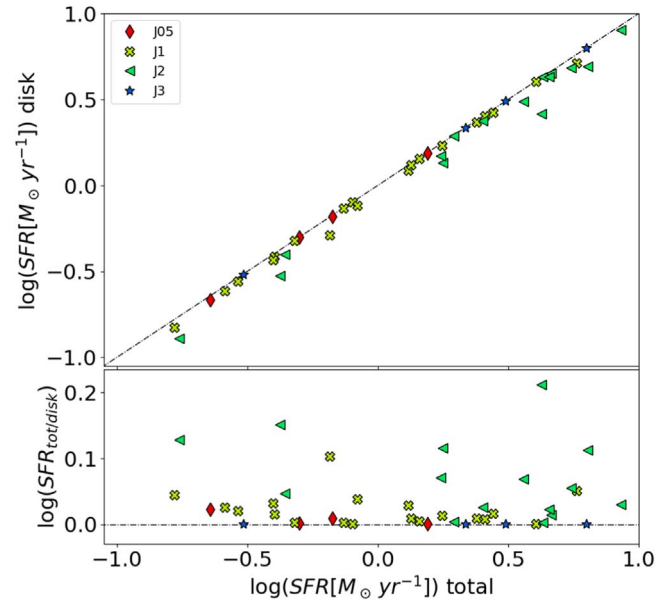


Figure 3. Comparison between the total and disk SFR. The upper panel compares the actual values, the lower panel shows the difference as a function of the total SFR. Dotted lines represent the loci where total and disk values coincide. Colors and symbols are as in Figure 1.

galaxies reduces the differences between stripping and control galaxies discussed in Figure 1, but fits are still different at $>1\sigma$ level and their difference is ~ 0.1 dex.

In contrast, most of the stripping galaxies have a measured SFR higher than that expected given the fit, with the results that their distribution is skewed toward higher values and is also broader. The standard deviation of the stripping sample is indeed ~ 1 , while that of the control sample is 0.4. The Kolmogorov–Smirnov test gives a high probability distributions are different (pvalue < 0.0001).

Both median and mean values are statistically different: $\Delta(\text{median}) = 0.15 \pm 0.01$, $\Delta(\text{mean}) = 0.22 \pm 0.01$. Note that the mean values are even more different because they are influenced by the tail of objects in the control sample with $\log(\text{SFR}_{\text{meas}}) - \log(\text{SFR}_{\text{fit}}) \sim -0.4$.

Having assessed that the SFR is enhanced in the disk, we can also investigate how much SF is found in the tails of the stripping galaxies. We remind the reader that in the control sample the amount of SF outside the disk is negligible and galaxies are located approximately on the 1:1 relation.

Figure 3 compares the total and disk SFR values of the stripping galaxies. As expected, in these galaxies the contribution of the SFR outside of the disk is conspicuous. The ratio between the total and disk SFR does not depend on the total SFR, indicating that the fraction of new stars produced in the tails is not strictly related to the total SFR. We do not detect a trend of the total and disk SFR with mass either (plot not shown). A dependence on the Jstage is instead observed: galaxies at the initial stripping and truncated disk have $\text{SFR}_{\text{tot}} \sim \text{SFR}_{\text{disk}}$, indicating no activity outside the disk. In contrast, in galaxies classified as J1 and J2, up to one-third of the total SFR can occur in the wake. Considering all classes together, the median log SFR difference between the two components is 0.02.

The differences between total and disk values are overall quite small, therefore the SFR– M_* relation obtained using the total values is not significantly different from the one presented in Figure 1 (plot not shown).

To conclude, our results show that in stripping galaxies, at any given mass, the SFR enhancement is already significant taking into account only the SF in the disk.

4. Summary and Conclusions

Exploiting the GASP data set, we have shown, for the first time in a statistically significant sample, that in observations stripping galaxies are characterized by a systematic enhancement of the SFR, compared to undisturbed galaxies of similar mass, indicating that SF is boosted in the disks during stripping. Additional SF takes place in the tails. We therefore confirm the results of Poggianti et al. (2016). Such enhancement had been already observed, but only in few individual cases (e.g., Crowl et al. 2006; Merluzzi et al. 2016; Kenney et al. 2014).

Due to otherwise low sample statistics, our control sample includes both cluster and field galaxies. Whether or not the SFR– M_* relation is dependent on environment, and by how much, is still a controversial topic. Results of, for example, Vulcani et al. (2010) and Paccagnella et al. (2016) showed that in cluster cores the relation is systematically shifted toward lower values, due to a population of galaxies with suppressed SF. Nonetheless, the bulk of the cluster population can be as star-forming as field galaxies (see also Poggianti et al. 2006). If, overall, the cluster relation is shifted low with respect to field galaxies, ours can be seen as a lower limit of the gap between stripping and undisturbed galaxies in clusters, and differences might be even more striking.

Our results suggest that RP moderately enhances the SF also in the central disk before removing the gas.

The triggering of SF in stripping galaxies has been debated in simulations, with different authors reaching quite different conclusions, as summarized in the Introduction. The origin of the enhancement is not clear yet, with some theoretical studies predicting a correlation with the cluster dynamical state. In future papers we will investigate the conditions in which SF triggering happens (relaxed or dynamically disturbed environment).

In M. Gullieuszik et al. (2018, in preparation) we will analyze whether the amount of mass and SF in the tails depends also on other factors, such as the cluster velocity dispersion, the position of the galaxy within the cluster, its orbit and its relative velocity with respect to the hosting system.

We thank the referee for their useful comments. Based on observations collected at the European Organization for Astronomical Research in the Southern Hemisphere under ESO programme 196.B-0578. We acknowledge funding from the INAF PRIN-SKA 2017 program 1.05.01.88.04. Y.J. acknowledges support from CONICYT PAI (Concurso Nacional de Inserción en la Academia 2017) No. 79170132.


ORCID iDs

Benedetta Vulcani  <https://orcid.org/0000-0003-0980-1499>

Bianca M. Poggianti  <https://orcid.org/0000-0001-8751-8360>

Marco Gullieuszik  <https://orcid.org/0000-0002-7296-9780>

Alessia Moretti  <https://orcid.org/0000-0002-1688-482X>

Stephanie Tonnesen  <https://orcid.org/0000-0002-8710-9206>

Jacopo Fritz  <https://orcid.org/0000-0002-7042-1965>

Daniela Bettoni  <https://orcid.org/0000-0002-4158-6496>

References

- Bekki, K. 2014, *MNRAS*, **438**, 444
- Bekki, K., & Couch, W. J. 2010, *MNRAS*, **408**, L11
- Bekki, K., Owers, M. S., & Couch, W. J. 2010, *ApJL*, **718**, L27
- Belfiore, F., Maiolino, R., Maraston, C., et al. 2016, *MNRAS*, **461**, 3111
- Bellhouse, C., Jaffé, Y. L., Hau, G. K. T., et al. 2017, *ApJ*, **844**, 49
- Boselli, A., Fossati, M., Gavazzi, G., et al. 2015, *A&A*, **579**, A102
- Calvi, R., Poggianti, B. M., & Vulcani, B. 2011, *MNRAS*, **416**, 727
- Cardelli, J. A., Clayton, G. C., & Mathis, J. S. 1989, *ApJ*, **345**, 245
- Chabrier, G. 2003, *PASP*, **115**, 763
- Consolandi, G., Gavazzi, G., Fossati, M., et al. 2017, *A&A*, **606**, A83
- Cortese, L., Marcillac, D., Richard, J., et al. 2007, *MNRAS*, **376**, 157
- Crowl, H. H., Kenney, J. D., van Gorkom, J. H., Chung, A., & Rose, J. A. 2006, *BAAS*, **38**, 1192
- Crowl, H. H., & Kenney, J. D. P. 2008, *AJ*, **136**, 1623
- Davies, L. J. M., Driver, S. P., Robotham, A. S. G., et al. 2016, *MNRAS*, **461**, 458
- Fasano, G., Marmo, C., Varela, J., et al. 2006, *A&A*, **445**, 805
- Fossati, M., Fumagalli, M., Boselli, A., et al. 2016, *MNRAS*, **455**, 2028
- Fritz, J., Moretti, A., Gullieuszik, M., et al. 2017, *ApJ*, **848**, 132
- Fujita, Y., & Nagashima, M. 1999, *ApJ*, **516**, 619
- Fumagalli, M., Fossati, M., Hau, G. K. T., et al. 2014, *MNRAS*, **445**, 4335
- Gavazzi, G., Consolandi, G., Belladitta, S., Boselli, A., & Fossati, M. 2018, *A&A*, **615**, 104
- Gullieuszik, M., Poggianti, B., Fasano, G., et al. 2015, *A&A*, **581**, A41
- Gullieuszik, M., Poggianti, B. M., Moretti, A., et al. 2017, *ApJ*, **846**, 27
- Gunn, J. E., & Gott, J. R., III 1972, *ApJ*, **176**, 1
- Jaffé, Y. L., Poggianti, B. M., Moretti, A., et al. 2018, *MNRAS*, **476**, 4753
- Jaffé, Y. L., Verheijen, M. A. W., Haines, C. P., et al. 2016, *MNRAS*, **461**, 1202
- Kapferer, W., Sluka, C., Schindler, S., Ferrari, C., & Ziegler, B. 2009, *A&A*, **499**, 87
- Kauffmann, G., Heckman, T. M., Tremonti, C., et al. 2003, *MNRAS*, **346**, 1055
- Kenney, J. D. P., Geha, M., Jáchym, P., et al. 2014, *ApJ*, **780**, 119
- Kennicutt, R. C., Jr. 1998, *ARA&A*, **36**, 189
- Kennicutt, R. C., Jr., Hao, C.-N., Calzetti, D., et al. 2009, *ApJ*, **704**, 1672
- Kewley, L. J., Heisler, C. A., Dopita, M. A., & Lumsden, S. 2001, *ApJS*, **132**, 37
- Kronberger, T., Kapferer, W., Ferrari, C., Unterguggenberger, S., & Schindler, S. 2008, *A&A*, **481**, 337
- McPartland, C., Ebeling, H., Roediger, E., & Blumenthal, K. 2016, *MNRAS*, **455**, 2994
- Merluzzi, P., Busarello, G., Dopita, M. A., et al. 2013, *MNRAS*, **429**, 1747
- Merluzzi, P., Busarello, G., Dopita, M. A., et al. 2016, *MNRAS*, **460**, 3345
- Moretti, A., Poggianti, B. M., Gullieuszik, M., et al. 2018, *MNRAS*, **475**, 4055
- Paccagnella, A., Vulcani, B., Poggianti, B. M., et al. 2016, *ApJL*, **816**, L25
- Poggianti, B. M., Fasano, G., Omizzolo, A., et al. 2016, *AJ*, **151**, 78
- Poggianti, B. M., Gullieuszik, M., Tonnesen, S., et al. 2018, *MNRAS*, submitted
- Poggianti, B. M., Jaffé, Y. L., Moretti, A., et al. 2017b, *Natur*, **548**, 304
- Poggianti, B. M., Moretti, A., Gullieuszik, M., et al. 2017a, *ApJ*, **844**, 48
- Poggianti, B. M., von der Linden, A., De Lucia, G., et al. 2006, *ApJ*, **642**, 188
- Quilis, V., Moore, B., & Bower, R. 2000, *Sci*, **288**, 1617
- Richards, S. N., Bryant, J. J., Croom, S. M., et al. 2016, *MNRAS*, **455**, 2826
- Roediger, E., & Brüggén, M. 2006, *MNRAS*, **369**, 567
- Roediger, E., Brüggén, M., Owers, M. S., Ebeling, H., & Sun, M. 2014, *MNRAS*, **443**, L114
- Roediger, E., & Hensler, G. 2005, *A&A*, **433**, 875
- Sharp, R. G., & Bland-Hawthorn, J. 2010, *ApJ*, **711**, 818
- Smith, R. J., Lucey, J. R., Hammer, D., et al. 2010, *MNRAS*, **408**, 1417
- Speagle, J. S., Steinhardt, C. L., Capak, P. L., & Silverman, J. D. 2014, *ApJS*, **214**, 15
- Steinhauser, D., Schindler, S., & Springel, V. 2016, *A&A*, **591**, A51
- Tonnesen, S., & Bryan, G. L. 2012, *MNRAS*, **422**, 1609
- Tonnesen, S., Bryan, G. L., & Chen, R. 2011, *ApJ*, **731**, 98
- Troncoso Iribarren, P., Padilla, N., Contreras, S., et al. 2016, *Galax*, **4**, 77
- Vijayaraghavan, R., & Ricker, P. M. 2013, *MNRAS*, **435**, 2713
- Vulcani, B., Poggianti, B. M., Finn, R. A., et al. 2010, *ApJL*, **710**, L1
- Yan, R., & Blanton, M. R. 2012, *ApJ*, **747**, 61